

COLOR IMAGE SEGMENTATION USING THE DEMPSTER-SHAFER THEORY OF EVIDENCE FOR THE FUSION OF TEXTURE

J. B. Mena, J.A. Malpica

Alcalá University, Escuela Politécnica, 28871, Alcalá de Henares, Madrid, Spain – juan.mena@uah.es

KEY WORDS: Color, Texture, Segmentation, Theory of evidence, Automatic extraction.

ABSTRACT:

We present a new method for the segmentation of color images for extracting information from terrestrial, aerial or satellite images. It is a supervised method for solving a part of the automatic extraction problem. The basic technique consists in fusing information coming from three different sources for the same image. The first source uses the information stored in each pixel, by means of the Mahalanobis distance. The second uses the multidimensional distribution of the three bands in a window centred in each pixel, using the Bhattacharyya distance. The last source also uses the Bhattacharyya distance, in this case cooccurrence matrices are compared over the cube texture built around each pixel. Each source represent a different order of statistic. The Dempster - Shafer theory of evidence is applied in order to fuse the information from these three sources. This method shows the importance of applying context and textural properties for the extraction process. The results prove the potential of the method for real images starting from the three RGB bands only. Finally, some examples about the extraction of linear cartographic features, specially roads, are shown.

1. INTRODUCTION

Segmentation of images represents a first step in many of the tasks that pattern recognition or computer vision has to deal with. There are many papers dealing with segmentation of images using color, see (Skarbek, 1994) for an early survey and (Cheng, 2001) for a more recent one. Several authors are applying different techniques for color in order to improve the final result of the segmentation, for example, (Park, 1998) presents a new algorithm based in mathematical morphology that performs a clustering in 3D color space; fuzzy techniques are applied by Yang et al. (Yang, 2002). Markov Random Fields are applied for clustering in (Jayanta, 2002).

Of the all possibilities for studying segmentation of color images in this paper we are going to focus on color texture. Texture is appealing for dealing with context information, so important in the psychological characteristics in recognising objects in images. Color textures have also studied by several authors, L. Song et al. (Song, 1996) have obtained the fractal dimension of color texture with the correlation among the color bands for feature extraction. Others that have used color and fractal dimension for color texture segmentation are A. Conci and C. B. Proenca (Conci, 1997). R. Krishnamoorthi and P. Bhattacharyya (Krishnamoorthi, 1997) have put forward an orthogonal polynomial base color texture model for the unsupervised segmentation of images with interesting results. The algorithms for the segmentation of images using color texture have a very broad field of application, such as clothing (Chang, 1996); automated surveillance (Paschos, 1999); retrieving of images from a large database (Zhong, 2000).

In this paper a new technique, called Texture Progressive Analysis (TPA), is presented. In this method color texture means using the interweaving of color information in the three bands by different order statistics. In order to obtain the greatest amount of information from the different order statistics, the method presented uses the theory of evidence (Shafer, 1976) as a fusion technique.

In section 2 the different order statistics will be presented. In section 3 the relationship between the systems RGB and HSI and the order statistics is applied. To fuse the information

coming from the three sources of information in the same image, the theory of evidence will be introduced in section 4. Finally some results with real images will be given in section 5 along with some conclusions.

2. THE SOURCES

Only color images have been considered in this work. Each image can be thought of as a set of points in a three dimensional euclidean space. Each pixel \mathbf{x} is represented as a point in this euclidean space, where the three coordinates could be RGB values or HSI values.

The training set is represented by several pixels in the area of interest. Let us call (\mathbf{m}_t, Σ_t) the mean and covariance matrix of the training set. For example, the training pixels used to segment the path in figure 2a) are shown in figure 2b).

In order to segment the image three order statistics have been used: In the first order statistic the Mahalanobis distance between pixels to be detected and the training set are used. In the second order a cooccurrence matrix that interweaves color bands is studied, and there is also an intermediate statistics which uses the Bhattacharyya distance between the distributions of pixels for the training area and the area to be detected.

2.1 Source 1: First order statistic

Since pixels are also points in a three dimensional space, the simplest way of classifying the pixels in the image, as belonging or not to the area of interest, would be to calculate the distance between the pixels to be classified and the training pixels. To see how far the new pixel is from the pixels in the area of interest it would be necessary to see how far the pixel in study \mathbf{x} is from \mathbf{m}_t of the training set. The Mahalanobis distance d (Fukunaga, 1990) will be used instead of the euclidean distance, since the former gives a better approximation than to the introduction of the covariance matrix. Its equation is:

$$d = (\mathbf{m}_t - \mathbf{x})^t \Sigma_t^{-1} (\mathbf{m}_t - \mathbf{x}) \quad (1)$$

where \mathbf{x} represents the pixel in study and (\mathbf{m}_t, Σ_t) are the mean and covariance matrix of the training set.

The result of applying the Mahalanobis distance to the detection of the path in the image in figure 2a) is presented in figure 2c). This last image represents the values obtained from the Mahalanobis distance normalized on a scale from 0 to 255. The brighter the pixel the closer it is to the training texture. In this case several pixels from the path area were taken as training pixels (figure 2b).

2.2 Source 2: One and a half order statistic

Instead of comparing (\mathbf{m}_t, Σ_t) with isolated pixels, as has just been done in the first order above, the group of pixels in the training set in this order statistic is going to be compared with the group of pixels around the pixel \mathbf{x} , to be analysed at that moment. This, in fact, is going to be established comparing the distribution of pixels in the training area, with the distribution of the pixels in an area around the pixel \mathbf{x} . In order to do that a window 5×5 has been taken around the pixel \mathbf{x} , which allow to calculate (\mathbf{m}_x, Σ_x) mean and covariance matrix for the distribution of the pixels in the window. We have called this the one and a half order statistics, since it is going to represent an intermediate state between the image obtained with the Mahalanobis distance and the one which is going to be obtained with the cube texture later on. If distributions of pixels in the window are close enough to the distribution of pixel in the training set then the central pixel in the window could be considered as belonging to the same group of the pixels in the training set. These distributions are compared using the Bhattacharyya distance b (Fukunaga, 1990):

$$b = \frac{1}{8}(\mathbf{m}_t - \mathbf{m}_x)^T \left(\frac{\Sigma_t + \Sigma_x}{2} \right)^{-1} (\mathbf{m}_t - \mathbf{m}_x) + \frac{1}{2} \log \frac{\frac{|\Sigma_t + \Sigma_x|}{2}}{\sqrt{|\Sigma_t| |\Sigma_x|}} \quad (2)$$

where Σ_x is the covariance matrix of the group of pixels in the window around the one in study \mathbf{x} . The result of applying the distance between distributions according to the function $\exp(-b)$, to the real image of figure 2a) is presented in figure 2d).

2.3 Source 3: Second order statistic. The texture cube

Pixels that are close together tend to be more related than pixels that are far away from each other. Statistics for pairs of pixels could be studied through many different techniques. We have looked for one that keeps the greatest amount of information with the minor complexity in terms of computing time.

The technique of cooccurrence matrices has shown its possibilities in many practical applications of textures. A long time ago J. Weszka et al. (Weszka, 1976) showed that cooccurrence matrices gave better results than spatial frequency methods for terrain classification. Gagalowicz (Gagalowicz, 1987) has shown the power of cooccurrence matrices for synthetic textures. He has also studied color and third order statistic, synthesising very complicated textures that requires a great amount of computing time for processing the images.

In order to obtain a robust method only the pixels that are less than three standard deviations from the media will be considered for the calculation of the mean and covariance matrix of the training set. Some pixels of the training set could be noise, or they could be not properly representing the texture for some reason. These pixels would be considered as outliers for the training set.

A model of color texture have been created similar to the one in Mao and Jain (Mao, 1992) in order to study the second order. We have tried to keep the major amount of information through out the whole process, using as few parameters as possible. Actually there are only two, the size of the window and the threshold for the plausibility that we will see in the following section. These two parameters are fixed for all the images so there is not necessity of tuning them for each picture, in that sense the process is without user intervention and therefore automatic.

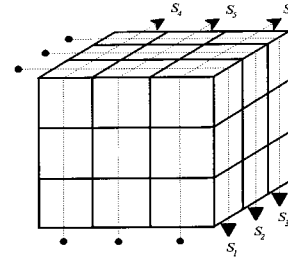


Figure 1. The texture cube

For each pixel \mathbf{x} a cube of edge three pixels is considered, as the one represented in figure 1. This cube is called *the cube texture*. The reason of fixing this size is to direct this method toward road extraction for a wide range of images. In fact, given the linear characteristics of roads, if a big window is used we run the risk of taking pixels outside the road.

First the three sections formed for the bands are considered, that is, each of the three sections S_k , $k = 1, 2, 3$. They correspond to each of the bands in the decomposition HSI of the image, where the pixel \mathbf{x} is in the centre position of the cube. The cube texture is formed with 27 cells, and since it has been consider 256 digital levels, each of the cells will have a number between 0 and 255. This has been done in this way, not using a threshold, in order to retain the maximum amount of information possible.

As a second step, three new sections from the cube texture will be considered, this time corresponding to the columns as shown in figure 1. Therefore there would be six sections altogether.

$$S_k = \begin{pmatrix} t_{11} & t_{12} & t_{13} \\ t_{21} & t_{22} & t_{23} \\ t_{31} & t_{32} & t_{33} \end{pmatrix}; \quad \begin{cases} k = 1, 2, \dots, 6 \\ t_{ij} \in [0, 255] \quad \forall i, j = 1, 2, 3 \end{cases} \quad (3)$$

For each section S_k , four cooccurrence matrices are built for each direction 0° , 45° , 90° and 135° . Therefore there are 24 matrices altogether. In fact, these matrices are not built directly for computing time reasons, since each matrix would have 65536 elements (256×256). The Section S_k is only of order three, therefore it would result in a sparse matrix with a high number of zeros. To avoid this, the cooccurrence distributions has suffer a minor modification that is showed as follow.

Let us be given the section S_k of pixel \mathbf{x} of equation (3). The cooccurrence distribution in the level of grey t_{ij} for the direction 0° is considered in the following manner:

$$DC_k[0^\circ] = \left\{ \begin{array}{l} (t_{11}, t_{12}), (t_{12}, t_{13}), (t_{13}, t_{21}), (t_{21}, t_{22}), \\ (t_{22}, t_{23}), (t_{23}, t_{31}), (t_{31}, t_{32}), (t_{32}, t_{33}) \end{array} \right\}$$

and similarly in the directions 45° , 90° and 135° .

Note that we enforce a sort of cyclic distributions, all built by eight elements with frequency equal to one. Therefore, the four directions shown above are symbolic. In this way the 65536 values of the cooccurrence matrix have been substituted by the pairs of cooccurrence which actually happen on the grey levels.

The features given in R. M. Haralick (Haralick, 1979) has been calculated from the 24 matrices constructed above. The features are these: Correlation, energy, entropy, maximum probability, contrast, and inverse difference moment. However, to avoid the problem of the sparsely in the matrices, as said before, the concept of pairwise probability has been modified in an ad hoc manner. Given the bidimensional distribution:

$$DC_{k[\alpha^{\circ}]} = \{(x_1, y_1), (x_2, y_2), \dots, (x_8, y_8)\}$$

we define the *pseudoprobability* of element (x_i, y_i) as:

$$ps_i = \frac{\sqrt{x_i y_i}}{8 \sum_{j=1}^8 \sqrt{x_j y_j}} \quad (4)$$

Then the values for the Haralick features are the following:

$$\begin{aligned} * \text{Correlation} : & \frac{1}{8} \sum_i \frac{(x_i - \bar{x})(y_i - \bar{y})}{\sigma_x \sigma_y} \\ * \text{Pseudoenergy} : & \sum_i ps_i^2 \\ * \text{Pseudoentropy} : & \sum_i ps_i \log ps_i \quad (5) \\ * \text{Maximum pseudoprobability} : & \text{Max}(ps_i) \\ * \text{Pseudocontrast} : & \sum_i |x_i - y_i| ps_i \\ * \text{Inverse difference pseudomoment} : & \sum_i \frac{ps_i}{|x_i - y_i|} \end{aligned}$$

For each \mathbf{x} a distribution of 24 vectors of dimension six (one for each Haralick feature) is obtained. This distribution (\mathbf{m}_x, Σ_x) is compared with the corresponding to the training set (\mathbf{m}_t, Σ_t) through the Bhattacharyya distance (2); then the respective value $exp(-b)$ is calculated. Figure 2e) shows the layer that is obtained after applying the texture cube technique to the image in 2a).

It appears that as the order of statistics increase the closer we are to the psychological concept of color detection. Some authors are using psychological concepts in automatic segmentation in order to improve some existing methods; such is the work done by Mirmehdi and Petrou (Mirmehdi, 2000).

After many trials with several images and under a visual evaluation we have chosen to apply:

- The RGB system in the first order statistics layer. It appears that results using HSI are not as good as with RGB.
- The HSI system in the intermediate layer. Though some results are regardless of which system is applied, RGB or HSI.

- The HSI system in the last layer, the texture layer. Here, the results using HSI are significantly better than applying RGB, therefore the former system has been applied.

3. FUSION OF THE INFORMATION LAYERS

The results obtained from the three techniques above give values that range between zero and one. This means that these values can be considered pieces of evidence for the recognition of the texture in study (Shafer, 1976).

We are going to consider only two classes in the Dempster-Shafer theory of evidence. Either a pixel belongs to the texture in study (to be detected) ω , or it belongs to the background ϖ . There is also an uncertainty θ inherent in the theory of evidence. All this constitute the frame of discernment Θ in our case.

$$\Theta = \{\omega, \varpi, \theta\}$$

For each pixel three values of evidence for each order statistic will be obtained $\mu_i (i=1,2,3)$

$$(\mu_i(\omega), \mu_i(\varpi), \mu_i(\theta)) \quad (6)$$

with the condition $\mu_i(\omega) + \mu_i(\varpi) + \mu_i(\theta) = 1, \forall i = 1,2,3$.

We will see that using the theory of evidence the three group of three values are fused to obtain only one group for each pixel.

3.1 The first order statistic

The Mahalanobis distances d (1) between pixel \mathbf{x} and the set of training pixels are calculated. Then the maximum d_{max} and minimum d_{min} values are obtained for normalising, and the complement to one is computed:

$$d' = 1 - \frac{d - d_{min}}{d_{max} - d_{min}} \quad (7)$$

The standard deviation for the distance's values for all the pixels obtained in (7) is taken as the uncertainty $\mu_1(\theta) = \sigma$. In order to verify the condition of summing equal to one, in equation (6), the values $\mu_1(\omega)$ are obtained in what follows:

$$\mu_1(\omega) = d'(1 - \sigma) \quad (8)$$

and by using its results the new evidence masses are obtained. These are the definitive values of evidence of each pixel of being close to the feature represented by the training set. Therefore the values for not belonging to the training set would be given by:

$$\mu_1(\varpi) = 1 - \mu_1(\omega) - \mu_1(\theta) = (1 - d')(1 - \sigma) \quad (9)$$

3.2 The first and a half and second order statistics

The Bhattacharyya distances b (2) between the training set (\mathbf{m}_t, Σ_t) and the window of each pixel (\mathbf{m}_x, Σ_x) are calculated. Then the corresponding values d' will be obtained by the following equation,

$$d' = \frac{1}{e^b} \quad (10)$$

Where b is the Bhattacharyya distance.

With the values d' the evidence masses are calculated with (8) and (9).

The standard deviation for the distances values is assigned to the uncertainty. $\mu_2(\theta) = \sigma$.

The second order statistic is calculated very similarly to the 1.5 order. Again the Bhattacharyya distance is used, and the evidence mass ω will be obtained by equation (10).

3.3 Orthogonal product and plausibility layer

With the values $\mu_i(\omega)$, $\mu_i(\varpi)$ and $\mu_i(\theta)$ for the three orders, $i=1, 2, 3$, the Dempster's rule or orthogonal product of the theory of evidence is applied (Shafer, 1976):

$$(\mu_i \otimes \mu_j)(A) = \frac{\sum_{B \cap C = A} \mu_i(B) \mu_j(C)}{\sum_{B \cap C \neq \phi} \mu_i(B) \mu_j(C)} ; (A, B, C \in \Theta) \quad (11)$$

where $A \cap \theta = A, \forall A \in \Theta$.

In our case the frame of discernment is quite simple $\Theta = \{\omega, \varpi, \theta\}$. It is useful to represent the orthogonal product with the following square of unit side:

	ω	ϖ	θ	$\rightarrow \mu_i$
ω	ω		ω	
ϖ		ϖ	ϖ	
θ	ω	ϖ	θ	
\downarrow				
μ_i				

One source μ_i is represented along one side, where the evidences ω, ϖ, θ , are given by their values. The other source μ_j is represented in the other side. The orthogonal product $\mu_i \otimes \mu_j$, for one element of the frame of discernment, is given by the sum of the rectangles inside of the square that has been label with this element.

Figure 2f) shows the layer that is obtained after applying the orthogonal product of the theory of evidence to the images in figure 2c), 2d) and 2e). Since the orthogonal product is associative a new set of masses is obtained by fusing the information coming from the three order of statistics: $\mu_f(\omega), \mu_f(\varpi), \mu_f(\theta)$, where $\mu_f = \mu_1 \otimes \mu_2 \otimes \mu_3$.

In order to give the final result of the segmentation a binary image is obtained showing which pixels belong to the texture and which do not. The concept of *plausibility* from the theory of evidence is applied. In our case the plausibility Π for the pixel x is the sum of the masses of the evidences for labelling the pixel as belonging to the training set plus the uncertainty, that is:

$$\Pi(x) = \mu_f(\omega) + \mu_f(\theta) = 1 - \mu_f(\varpi) \quad (12)$$

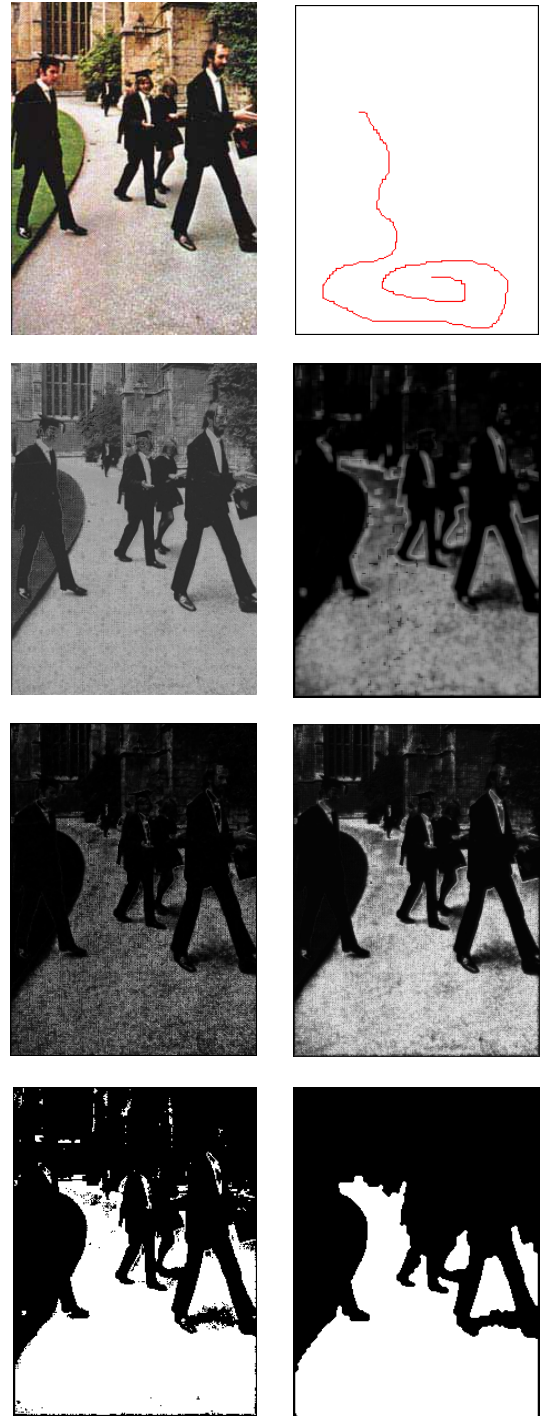


Figure 2. (Up to down and left to right): a) Original image. b) Training set. c) First order layer. d) First and a haft order layer. e) Second order layer. f) Evidence masses. g) Plausibility layer. h) Clean plausibility layer.

Here it is necessary to define a threshold in order to proceed with the segmentation. As said above, it can be observed this is one of the few parameters of the algorithm. It is the more relevant since it could not be guarantee that an optimal segmentation would be obtained in all cases. In figure 2g) is represented the binary image obtained, and the figure 2h) presents the image result after a clean process of small noise areas, with the only objective of a better visualisation.

4. RESULTS, EVALUATION AND CONCLUSIONS

4.1 Other results obtained

The process explain with the image of figure 2, has been followed with many images, in all cases the results obtained with the fusion of information from the different order of statistics have been better than the ones obtained only with information from the first order of statistic (Mahalanobis distance). Some of these images are shown in the following figures: The figure 3 shows the binary segmentation of the woman's dress; the figure 4 presents the extraction of the lake on a terrestrial image; and the figures 5, 6, 7 and 8 present the application of our method in the automatic road extraction on aerial and satellite images.

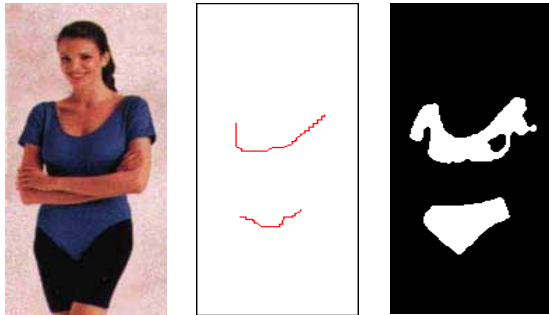


Figure 3. (Left to right): Original terrestrial image. Training set. Automatic result.



Figure 4. (Left to right): Original terrestrial image. Training set. Automatic result.

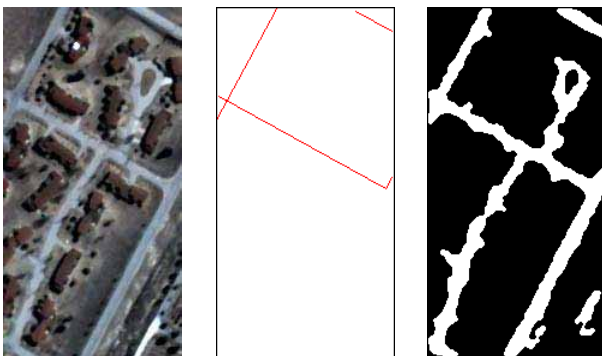


Figure 5. (Left to right): Original IKONOS satellite image. Training set. Automatic result.



Figure 6. (Left to right): Original aerial image. Training set. Automatic result.

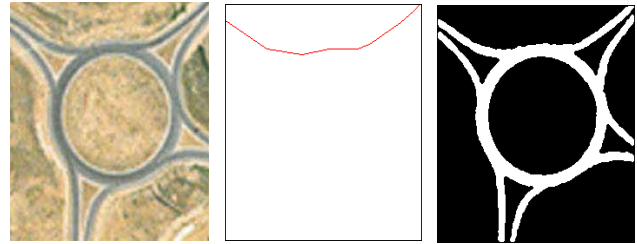


Figure 7. (Left to right): Original aerial image. Training set. Automatic result.

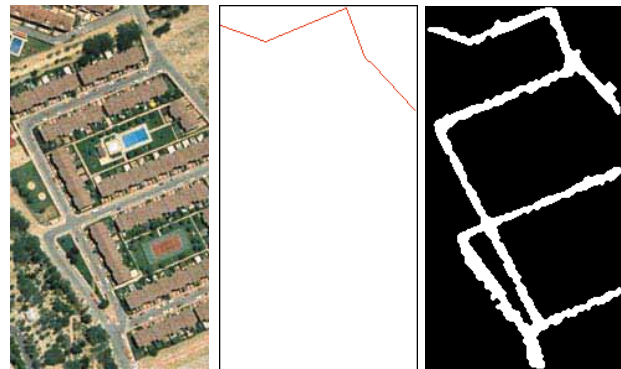


Figure 8. (Left to right): Original aerial image. Training set. Automatic result.

4.2 Evaluation

The first source has the disadvantage with reference to the second or third source (higher statistical order) that the results dependent on the training set chosen. However, when information from the first source is mixed with the information from the other layers using the theory of evidence this problem is partially solved. This is the principal advantage of our system. When the second order statistic classifier fails to recognise a pixel as belonging to the training area, the mixer of information of the layers with lower order statistics compensate for the miscalculation. To summarise, the mixing of information through the orthogonal product produces better results than those obtained using only just one order statistics, being immaterial of whether it is the first, the second or the third sources.

In order to check the efficiency of our method, the comparison of TPA technique with the known Mahalanobis classifier is presented in table 1 on diverse types of imagery. For each of images 2 to 5, in the first row of each box; it shows the percent of correct pixels detected for the first source only, and the corresponding percent for the method developed with the TPA.

The percents of errors type 1 (pixels erroneously detected) and type 2 (pixels no detected) are presented in the other rows for both methods.

	MAHALANOBIS CLASSIFIER TECHNIQUE	TEXTURE PROGRESSIVE ANALYSIS	
Correctness	90.68	95.15	Fig 2
Errors type 1	8.69	1.47	
Errors type 2	0.63	3.38	
Correctness	83.82	92.54	Fig 3
Errors type 1	15.95	0.16	
Errors type 2	0.23	7.31	
Correctness	63.27	99.63	Fig 4
Errors type 1	36.64	0.09	
Errors type 2	0.09	0.28	
Correctness	71.33	93.88	Fig 5
Errors type 1	28.28	4.02	
Errors type 2	0.39	2.09	

Table 1. Comparison between TPA technique and Mahalanobis classifier.

About the automatic road extraction, the evaluation of our system is achieved through an approach to the Wiedemann method, presented in the paper (Wiedemann, 1998). The corresponding central axis of the results are then compared with the manual extraction, obtaining the values presented in table 2 on images 5, 6, 7 and 8.

Measures	5	6	7	8	Mean
Resolution (m)	1	2	1	2	1.5
Completeness (%)	79	66	86	91	81
Correctness (%)	82	65	93	94	84
Quality (%)	67	48	81	87	71
RMS difference(m)	0.6	1.2	0.6	1.2	0.9
Redundancy	0.004	0.01	0.02	0.01	0.01
Gaps per Km.	0	0	0	0	0.0
Gap length (m)	0	0	0	0	0.0

Table 2. Evaluation on road extraction.

4.3 Conclusions

Herein we have proposed a new method in order to extract automatically information on terrestrial, aerial and satellite images. The segmentation process is especially important for solving the problem of thematic mapping with use of remote sensing data, since a binary image of high quality is essential for solving the later raster-vector conversion.

One of the major advantages of the technique described in this paper is that it needs only a few parameters, and most of the information is retained until the very end. These few parameters are fix throughout out the whole algorithm and are the same for all the pictures so the process could be considered almost automatic, therefore it is proved that the introduction of information of high order of statistics is good in all the cases.

At the end, the principal advantage of our approach is the decreasing of the manual work in the process of bringing up to date of data bases, geographical or other type, starting from a minimum of input data.

5. REFERENCES

- Chang, C. C., L. L. Wang, 1996. Color texture segmentation for clothing in a computer-aided fashion design system. *Image and Vision Computing*, 14(9), pp. 685-702.
- Cheng, H. D., X. H. Jiang, Y. Sun, Jingli Wang, 2001. Color image segmentation: advances and prospects. *Pattern Recognition*, 34, pp. 2259-2281.
- Conci, A., C.B. Proenca, 1997. A box-counting approach to color segmentation. *Proc. Int Conf on Image Processing, IEEE Comput. Soc, Los Alamitos, California*, pp. 228-230.
- Fukunaga, K., 1990. *Statistical Pattern Recognition*. Academic Press, Second Ed.
- Gagalowicz, A., 1987. Texture modelling applications. *The Visual Computer*, Springer Verlag, 3, pp. 186-200.
- Haralick, R. M., 1979. Statistical and Structural Approaches to Texture. *Proc. IEEE*, 67(5), pp. 786-804.
- Jayanta, M., 2002. MRF clustering for segmentation of color images. *Pattern Recognition Letters*, 23(8), pp. 917-929.
- Krishnamoorthi, R., P. Bhattacharyya, 1997. On unsupervised segmentation of color texture images. *Proc. Fourth Int Conf on High-Performance Computing, IEEE Computer. Soc Press, Los Alamitos, California*, pp. 500-504.
- Mao, J., A. K. Jain, 1992. Texture Classification and Segmentation Using Multiresolution Simultaneous Autoregressive Models. *Pattern Recognition*, 25(2), pp. 173-188.
- Mirmehdi, M., M. Petrou, 2000. Segmentation of color texture. *IEEE Trans. Pattern Analysis and Machine Intelligence*, 22(2), pp. 142-158.
- Park, S., Il Dong Yun, Sang Uk Lee, 1998. Color image segmentation based on 3-D Clustering: Morphological approach. *Pattern Recognition*, 31(8), pp. 1061-1076.
- Paschos, G., F.P. Valavanis, 1999. A color texture based visual monitoring system for automated surveillance. *IEEE Transactions on Systems, Man and Cybernetics*, 29(2), pp. 298-307.
- Shafer, G., 1976. *A Mathematical theory of Evidence*. Princeton University Press, Princeton, NJ.
- Skarbek, W., A. Koschan, 1994. Color Image Segmentation. Report, Technical University, Berlin.
- Song, L., Y. Ruikang, I. Saarinen, M. Gabbouj, 1996. Use of fractals and median type filters in color texture segmentation. *Proc. IEEE International Symposium on Circuits and Systems. Circuits and Systems Connecting the World*, New York, USA, pp. 108-111.
- Weszka, J., C. Dyer, A. Rosenfeld, 1976. A comparative study of texture measures for terrain classification. *IEEE Trans. Syst., Man, and Cybern*, 6(4), pp. 269-285.
- Wiedemann, C., C. Heipke, H. Mayer, O. Jamet, 1998. Empirical evaluation of automatically extracted road axes. In: *Empirical Evaluation Methods in Computer Vision*, Kevin J. Bowyer, P. Jonathon Phillips (Editors), *IEEE Computer Society Press* pp 172-187. Also in: *9th Australasian Remote Sensing and Photogrammetry Conference, The University of New South Wales, Sydney*, Paper No. 239 (CD).
- Yang, J. F., Shu-Sheng Hao, Pau-Choo Chung, 2002. Color image segmentation using fuzzy C-means and eigenspace projections. *Signal Processing*, 82(3), pp. 461-472.
- Zhong, Y., A. K. Jain, 2000. Object location using color texture and shape. *Pattern Recognition*, 33(4), pp. 671-684.
- Zugaj, D., V. Lattuati, 1998. A new approach of color images segmentation based on fusing region and edge segmentations outputs. *Pattern Recognition*, 31(2), pp. 105-113.